Structures of Energetic Acetylene Derivatives $HC{\equiv}CCH_2ONO_2$, $(NO_2)_3CCH_2C{\equiv}CCH_2C(NO_2)_3$ and Trinitroethane, $(NO_2)_3CCH_3$

Thomas M. Klapötke[a], Burkhard Krumm[a], Richard Moll[a], Alexander Penger[a], Stefan M. Sproll[a], Raphael J. F. Berger[b], Stuart A. Hayes[b], and Norbert W. Mitzel[b]

[a] Department of Chemistry, Ludwig-Maximilian University of Munich, Butenandtstraße 5 – 13 (D), 81377 Munich, Germany

[b] Inorganic and Structural Chemistry, Bielefeld University, Universitätsstraße 25, 33615 Bielefeld, Germany

Reprint requests to Prof. Dr. Thomas M. Klapötke. Fax: +49-89-2180-77492.
E-mail: tmk@cup.uni-muenchen.de

Z. Naturforsch. **2013**, *68b*, 719 – 731 / DOI: 10.5560/ZNB.2013-2311
Received November 27, 2012

Dedicated to Professor Heinrich Nöth on the occasion of his 85th birthday

The molecular structures and relative ratios of the two conformers (*anti* and *gauche*) of $HCCCH_2ONO_2$ detected in the gas phase at room temperature have been determined by electron diffraction. The results are discussed on the basis of quantum chemical calculations. The molecular structures of $(NO_2)_3CCH_2C{\equiv}CCH_2C(NO_2)_3$ and $(NO_2)_3CCH_3$ have been determined by X-ray diffraction. A ^{109}Ag NMR study was performed for silver trinitromethanide $Ag[C(NO_2)_3]$ in various polar solvents.

Key words: Gas-phase Electron Diffraction, X-Ray Diffraction, High Energy Dense Oxidizer, Trinitromethyl, Silver NMR

Introduction

The research of energetic materials is driven by the goal to obtain materials with superior properties, but it is also highly desirable to generate a better understanding of well described systems. Among the class of energetic nitrate esters, nitroglycerine and nitrocellulose are well established liquid propellant systems and smokeless powders, whereas pentaerythritol tetranitrate is a powerful explosive. Low molecular weight nitrate esters like methyl nitrate, designated as MYROL in WWII, have been widely discussed as components for liquid rocket engines [1]. Unfortunately, all nitrate esters tend to show extreme sensitivities towards shock and impact, which is a result of adiabatic compression and consequently local overheating [2, 3].

The combination of oxidizing groups with an organic backbone as fuel is a common approach for designing new energetic materials. Surprisingly, energetic compounds based on the highly endothermic acetylene are rare in the literature. However, butin-2-diol-1,4-dinitrate has been investigated and shown to be more sensitive than nitroglycerine [4]. Another member of acetylenic energetic materials is propargyl nitramine, which has been discussed due to its high specific impulse of $I_{sp} = 233$ s as a liquid monopropellant for rocket motors [5]. The high volatility limits its usage for standard applications drastically, but opens possibilities for structural investigations in the gas phase. The related propargyl azide was investigated by means of gas-phase electron diffraction (GED). Its hydrocarbon skeleton has been found to adopt a *gauche* conformation with respect to the azide group [6].

Earlier reports have shown that the reaction of acetylenes with HNO_3 can result in the formation of isoxazole heterocycles [7 – 12]. Propargyl nitrate, $HC{\equiv}CCH_2ONO_2$ (**1**), among other acetylene and diacetylene alcohols, has been prepared by nitration of propargyl alcohol [13], but only poorly characterized. Hexanitrohex-3-yne, $(NO_2)_3CCH_2C{\equiv}CCH_2C(NO_2)_3$ (**2**), another known energetic acetylene derivative, has also been only insufficiently described and characterized [14]. In addition, for **2** the results of theoretical studies predicting impact sensitivities have been

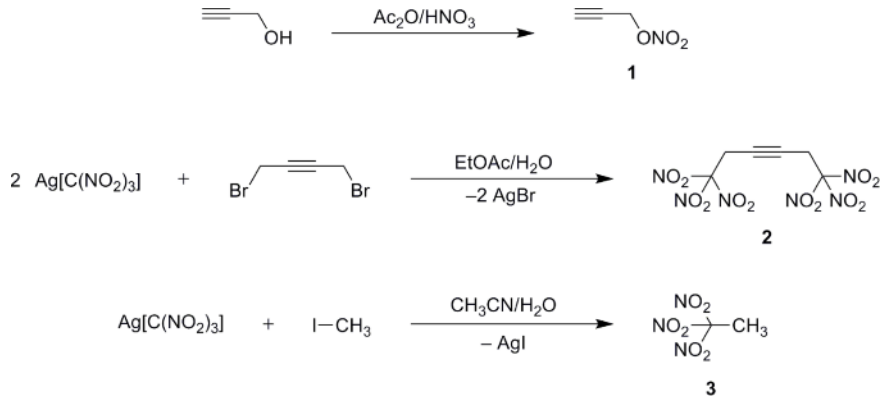

Scheme 1. Synthesis of compounds **1**–**3**.

reported [15 – 19]. 1,1,1-Trinitroethane, $(NO_2)_3CCH_3$ (**3**), was first briefly mentioned in 1886 [20]. Further work on **3** was performed together with the discovery of silver trinitromethanide used as a starting material [21]. Some mechanistic studies on the synthesis of **3** by the alkylation reaction using silver trinitromethanide and methyl iodide followed [22]. This synthesis and its kinetics have been further investigated more than half a century later [23]. Various formation reactions of **3** have been reported [21, 24 – 26], as well as some characterization using NMR spectroscopy [26 – 30], vibrational spectroscopy [31, 32] and mass spectrometry [33 – 35]. Apart from some basic theoretical predictions of its molecular geometry [22, 36], structural studies of **3** using X-ray diffraction have not been undertaken so far (*cf.* our initial results displayed in [37]).

In this contribution, the results of a detailed study of the synthesis and characterization of propargyl nitrate (**1**), 1,1,1,6,6,6-hexanitrohex-3-yne (**2**), and 1,1,1-trinitroethane (**3**) are presented.

Results and Discussion

Synthesis and spectroscopic characterizations

Propargyl nitrate (**1**) was synthesized by using the well-established nitration system Ac_2O/HNO_3 (100 %). Due to its high volatility, the gas phase structure could be determined by means of gas electron diffraction (GED) along with quantum chemical calculations. The synthesis of 1,1,1,6,6,6-hexanitrohex-3-yne (**2**) and 1,1,1-trinitroethane (**3**) was performed by alkylation reactions of silver trinitromethanide with the appropriate aliphatic halides (Scheme 1). The driving force of this reaction, which works even at ambient temperature, is the affinity of the silver cation to heavier halide ions, *i. e.* the formation of silver bromide for **2** and silver iodide for **3**. By contrast, the reactions of 1,4-dibromobut-2-yne or iodomethane with potassium trinitromethanide did not yield a product, although a very slow reaction of iodomethane with potassium trinitromethanide in acetone has earlier been reported [38, 39]. The progress and extent of the formation of **2** and **3** can be conveniently followed by filtering and weighing the precipitated silver halides. Previous kinetic and mechanistic investigations of silver salts with alkyl halides have supported a mechanism which has both S_N1 and S_N2 character [23, 40]. The alkylation can proceed in two directions, either by C- or O-alkylation. It was found that the formation of unstable O-alkylated products is predominant for many halides other than primary halides [23, 41 – 43]. The alkylation of silver trinitromethanide to form **2** and **3** leads primarily to the desired C-alkylated products, due to the lack of stabilization of a S_N1-type transition state [22, 42]. Solvent effects on alkylation reactions of silver trinitromethanide have earlier been investigated [23].

To achieve a successful synthesis and a high conversion rate, silver trinitromethanide should be freshly prepared and be used *in situ*. The presence of water stabilizes silver trinitromethanide against decomposition to silver nitrate and nitrogen oxides. Otherwise, silver nitrate would react more rapidly with alkyl halides than silver trinitromethanide, to form nitrate esters and not the desired trinitromethyl derivatives [23]. In this context it should be noted that only reports on the crys-

Table 1. ^{109}Ag and ^{14}N NMR data of silver trinitromethanide (in ppm).

Solvent	$Ag[C(NO_2)_3]$	
	δ ^{109}Ag	δ ^{14}N
D_2O	27.5	−33
[D_4]Methanol	48.8	−24
[D_6]Acetone	108.4	−20
[D_6]DMSO	181.1	−30
[D_3]Acetonitrile	429.7	−29

tal structure of silver trinitromethanide as a mono- or hemihydrate have been published [22, 44]. The decomposition mechanism is analogous to that of the corresponding potassium salt [21, 23]. The synthesis of silver trinitromethanide described in the literature uses moist silver oxide and trinitromethane [21, 23, 44]. It was found in this work that the use of silver carbonate or acetate instead is more convenient due to more facile work-up and increased yields. Both reactions can be performed in water or acetonitrile as solvents.

The solubility of $Ag[C(NO_2)_3]$ in several polar solvents enabled ^{109}Ag and ^{14}N NMR studies and showed that the NMR chemical shift is highly dependent on the nature and polarity of the coordinating solvent (Table 1). This is due to the formation of silver complexes with electron donating solvents [23, 45], which results in significant shifts of the ^{109}Ag and, to some extent, the ^{14}N NMR resonances. Similar large shielding variations have been observed in ^{109}Ag NMR spectra of silver halides in S/N/O-bonded ligands, but not, as in this case, to a complex anion, such as the trinitromethanide anion [46].

Gas-phase structure analysis

GED structure models

Two conformers of **1** (*gauche* and *anti*, Fig. 1) differing with respect to the dihedral angle N6/N16–O5/O15–C4/C14–C3/C13 have been included into the structure refinement model. Based on the results of quantum chemical calculations the following assumptions were made: For both conformers planarity of the NO_3 moieties, linearity of the HCCC moieties and equal C–H distances; moreover, C_s symmetry was assumed for the *anti*-conformer. The remaining degrees of freedom to describe the molecular structures of both conformers were chosen as the following set of primitive internal coordinates: H1–C2, C2≡C3, C3–C4, C4–H9, C4–H10, C4–O5, O5–N6, N6=O8, N6=O7 (bonded lengths); O8–N6–O5, O8=N6=O7, N6–O5–C4, H9–C4–H10; H9–C4–$H10_{rock}$, H9–C4–$H10_{twist}$ H9–C4–$H10_{wagg}$ (angles; *rock*-, *twist*- and *wag*-angular degrees of freedom are defined according to the nomenclature for vibrational spectroscopy [47]; the deviations of these angles refer to the fully regular tetrahedral configuration); N6–O5–C4–C3, O8–N6–O5–C4 (torsions); and the respective internal coordinates for the *anti*-conformer. In agreement with the C_s symmetry constraint in the *anti*-conformer, the H19–C14–$H20_{rock}$ and the H19–C14–$H20_{twist}$ angles were fixed to 0°, the N16–O15–C14–C13 dihedral angle was set to 180°, and the O18–N16–O15–C14 dihedral angle was set to 0°.

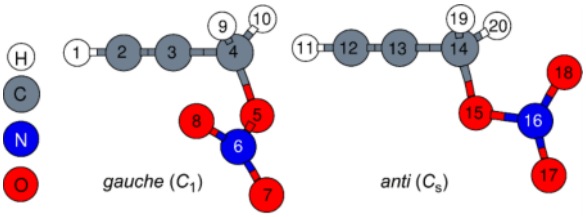

Fig. 1. Molecular structures of *gauche*- and *anti*-$HCCCH_2ONO_2$ (**1**), showing the atom numbering scheme used for the GED structure refinement.

GED structure refinement

Due to the occurrence of two conformations of **1** (Fig. 1) in significant amounts and a subset of structure parameters corresponding to bonded interatomic distances similar in size, inter-parameter correlation in the least-squares refinement procedure has to be expected. In order to circumvent correlation problems to some extent, problem adapted combinations of internal coordinates were formed. The general strategy for such a procedure has previously been outlined [48]. For example, the three short bonded inter-heavy-atom-distances C2≡C3, N6=O8, and N6=O7 (given in increasing size according to the calculated values) were transformed into the three problem adapted linear combinations $rXX^{s}_{m1}{}^{gauche}$ = (C2≡C3 + N6=O8 + N6=O7)/3, $rXX^{s}_{m2}{}^{gauche}$ = (C2≡C3 − N6=O7)/2 and $rXX^{s}_{m3}{}^{gauche}$ (C2≡C3 – 2 × N6=O8 + N6=O7). For the *anti*-conformer similar parameters were defined ($rXX^{s}_{m1}{}^{anti}$, $rXX^{s}_{m2}{}^{anti}$, $rXX^{s}_{m3}{}^{anti}$). Moreover, corresponding parameters in the two different conformers of **1** (*anti* and *gauche*) were

Table 2. Independent parameters[a] used in the GED refinement of **1** (refined parameter values, calculated values obtained at the SCS-MP2/TZVPP level of theory, and applied restraints).

	Parameter description	GED r_a	GED $r_{a3,1}$	MP2 r_e	Restraint uncertainty[b]
p_1	*d* N6–O5–C4–C3	83.8(9)	86(1)	77.3	∞
p_2	*d* O7–N6–O5–C4	168(1)	168(2)	–175.1	∞
p_3	rXX^{s}_{m1} average (*gauche, anti*)	1.203(1)	1.2015(9)	1.1943	∞
p_4	rXX^{s}_{m1} diff. (*gauche, anti*)	0.0013(1)	0.00130(8)	0.00133	0.0001
p_5	rXX^{l}_{m1} average (*gauche, anti*)	1.447(1)	1.435(1)	1.427	∞
p_6	rXX^{l}_{m1} diff. (*gauche, anti*)	−0.009(1)	−0.008(8)	−0.003	∞
p_7	rXX^{s}_{m2} average (*gauche, anti*)	0.005			0
p_8	rXX^{s}_{m2} diff. (*gauche, anti*)	0.0			0
p_9	rXX^{l}_{m2} average (*gauche, anti*)	0.023(6)	0.024(6)	0.026	∞
p_{10}	rXX^{l}_{m2} diff. (*gauche, anti*)	0.0025			0
p_{11}	rXX^{s}_{m3} average (*gauche, anti*)	−0.03(3)	−0.03(3)	−0.01	∞
p_{12}	rXX^{s}_{m3} diff. (*gauche, anti*)	−0.008			0
p_{13}	rXX^{l}_{m3} average (*gauche, anti*)	−0.05(2)	−0.03(2)	0.02	∞
p_{14}	rXX^{l}_{m3} diff. (*gauche, anti*)	−0.029			0
p_{15}	[∠(O18–N16–O17) + ∠(O8–N6–O7)]/2	132.0(7)	131.3(8)	130.1	∞
p_{16}	[∠(O18–N16–O17) − ∠(O8–N6–O7)]/2	−0.3			0
p_{17}	[∠(O15–N16–O17) + ∠(O5–N6–O7)]/2	111.8(8)	112.7(6)	112.6	∞
p_{18}	[∠(O15–N16–O17) − ∠(O5–N6–O7)]/2	0.4			0
p_{19}	[∠(N16–O15–C14) + ∠(N6–O5–C4)]/2	114.4(4)	112.4(4)	113.1	∞
p_{20}	[∠(N16–O15–C14) − ∠(N6–O5–C4)]/2	0.0			0
p_{21}	[∠(O15–C14–C13) + ∠(O5–C4–C3)]/2	107.7(4)	109.4(5)	108.2	∞
p_{22}	[∠(O15–C14–C13) − ∠(O5–C4–C3)]/2	−2.6			0
p_{23}	*r*CH average (CH_2, CH)	1.097(6)	1.095(5)	1.099	0.01
p_{24}	*r*CH diff. (CH_2, CH)	0.0275			0
p_{25}	∠CH_2	108.2			0
p_{26r}	*rock* (CH_2, *gauche*)	2.8			0
p_{27}	*twist* (CH_2, *gauche*)	3.9			0
p_{28}	*wagg* (CH_2, *gauche*)	−16.8			0
p_{29}	*fraction*(*anti*)	69(2) %	69(2) %	70 %[c]	∞
	R factor (R_G)	8.08 %	8.72 %	–	–

[a] All distances are in Å, and angles are in degrees. The two sets of parameter values for the GED refinement, r_a and r_e, correspond to different approaches accounting for vibrational motion. The r_a structure is based on harmonic thermal average distances, whilst the $r_{a3,1}$ structure is an approximation to an equilibrium structure r_e based on a computed (DFT, see Experimental Section) cubic molecular force field [51–53]; [b] "0" for unrefined (= fixed) values, "∞" for freely refined (unrestrained); [c] estimated from $k = \exp(-\Delta E/RT)$, R = 8.314 J mol^{-1} K^{-1}), $T = 293$ K, $\Delta E = -0.55$ kcal mol^{-1} (from the SCS-MP2/TZVPP calculation).

transformed into a set of average and difference parameters, for example: p_{15} = (O8=N6=O7 + O18=N16=O7)/2 and p_{16} = (O8=N6=O7 − O18=N16=O7)/2 or $p_3 = (rXX^{s}_{m1}{}^{gauche} + rXX^{s}_{m1}{}^{anti})/2$ and $p_4 = (rXX^{s}_{m1}{}^{gauche} - rXX^{s}_{m1}{}^{anti})/2$. The resulting set of independent parameters, together with the refined values and applied restraints and constraints is given in Table 2. The refinement was performed according to the SARACEN method [49, 50], which places flexible restraints on parameters that are not well resolved from the GED experiment, with the value of the restraint and the uncertainty estimated from calculated values.

The experimental molecular intensity and radial distribution curves are shown in Figs. 2 and 3, with the refined difference curves at the bottom of each figure.

Amplitudes of vibration were also refined for both molecules, but those corresponding to distances under a single peak in the respective radial-distribution curve (RDC, see Fig. 3) were grouped together by fixing relative amplitude ratios. Restraints of 10 % of the calculated values were applied to the refined reference amplitudes. The full lists of inter-atomic distances, amplitudes of vibration and distance corrections for the $r_{a3,1}$ refinements, including details of which ampli-

Table 3. Structure parameters from the GED refinement of *anti*- and *gauche*-$HCCCH_2ONO_2$ and calculated values obtained at the HF/ and SCS-MP2/TZVPP level of theory. Distances are given in Å, angles in degrees.

Dependent parameter	GED $r_{a3,1}$	GED r_a	MP2 r_e	HF r_e
N6–O7	1.191(6)	1.194(5)	1.201	1.167
N6–O8	1.211(10)	1.214(9)	1.206	1.176
C2–C3	1.201(6)	1.204(5)	1.212	1.180
N6–O5	1.413(6)	1.427(6)	1.423	1.336
C4–O5	1.445(5)	1.459(5)	1.439	1.424
C3–C4	1.458(11)	1.466(10)	1.463	1.464
C3–C4–O5	110.7(5)	110.3(4)	112.6	112.7
C4–O5–N6	112.4(4)	113.7(3)	112.8	116.7
O5–N6–O7	112.4(9)	111.3(8)	112.1	113.5
O5–N6–O8	116.2(3)	116.8(3)	117.3	118.0
O7–N6–O8	131.5(8)	131.9(7)	130.6	128.5
N16–O17	1.191(6)	1.194(5)	1.201	1.167
N16–O18	1.215(10)	1.218(9)	1.209	1.179
C12–C13	1.201(6)	1.204(5)	1.211	1.197
N16–O15	1.398(7)	1.408(6)	1.414	1.331
C14–O15	1.447(9)	1.456(9)	1.446	1.430
C13–C14	1.448(7)	1.452(6)	1.459	1.460
C13–C14–O15	108.1(5)	107.7(5)	105.8	106.6
C14–O15–N16	112.4(4)	113.7(3)	112.0	115.4
O15–N16–O17	112.8(9)	111.7(8)	112.5	117.8
O15–N16–O18	116.1(3)	116.7(3)	117.3	113.9
O17–N16–O18	131.2(8)	131.6(7)	130.2	128.4

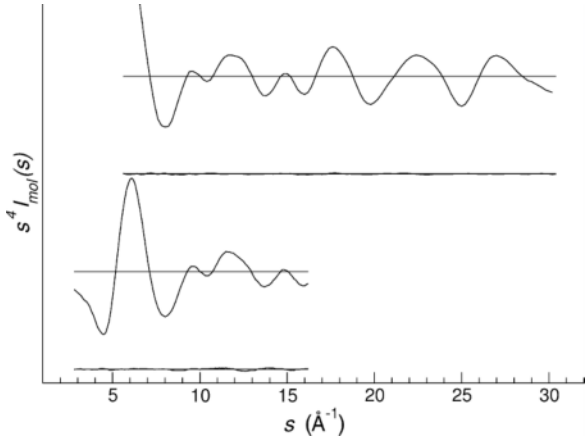

Fig. 2. Experimental and difference (experimental minus theoretical) molecular intensity curves for **1**.

tudes were kept at fixed ratios and which were refined, are provided as Supporting Information.

The refinement of the structure of **1** yielded a good fit of the experimental to the theoretical intensities for both the r_a and $r_{a3,1}$ structure types, as can be seen from the low R_G factors of 8.1 % and 8.7 %, (Tables 2 and 3) respectively. The quality of the fit can also be judged

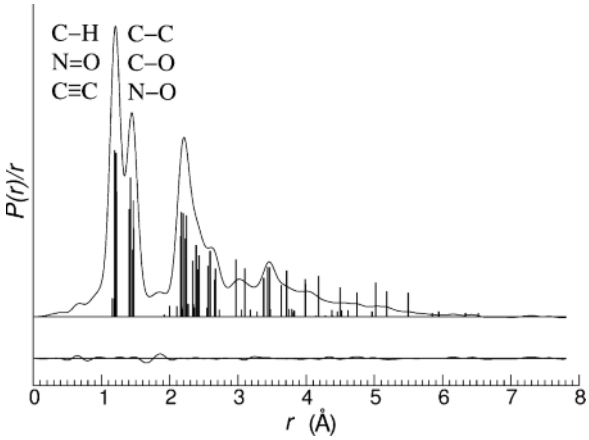

Fig. 3. Experimental and difference (experimental minus theoretical) radial distribution curves for **1**.

by the appearance of the molecular intensity and radial distribution curves (Figs. 2 and 3).

Discussion of gas-phase geometries

The ratio of the *anti*-conformer to the total amount of compound under the conditions of the GED experiment was refined to 69(2) %, which is in agreement with the calculated *ab initio* total energy difference of 0.6 kcal mol^{-1} (*gauche-anti*, SCS-MP2/TZVPP). A selection of the important geometrical parameters from the GED structure refinement and the corresponding values determined in the *ab initio* calculations are displayed in Table 3. GED parameters are given in terms of both the r_a and $r_{a3,1}$ structure types. The inter-nuclear distance obtained directly from the GED data, r_a, is the harmonic mean and can be converted to the arithmetic mean, r_g, using the root-mean-squared amplitude of vibration, u: $r_g \approx r_a + u^2/r$. Distance corrections, k, are regularly applied in GED refinements to account for the 'shrinkage' effect. When the vibrational motion is considered to be harmonic with curvilinear trajectories, the resulting distances and distance corrections are termed r_{h1} and k_{h1}, respectively. Comparison of the calculated values indicates that the alkyne and methylene groups are well described by HF theory, with only small changes in the values of these parameters as the theoretical treatment is improved by way of MP2 theory. In contrast, the HF model appears to have severe limitations with regard to the treatment of the nitrate group. The ter-

minal N–O bonds are significantly elongated upon introduction of a MP2 correction by about 3 pm when the geometries calculated with identical basis sets are compared. The largest discrepancy between the HF and MP2 geometries is in the length of the N6–O5 bond, which increases by 0.09 Å.

X-Ray structure determinations

Single crystals suitable for X-ray diffraction measurements were obtained by crystallization at lower temperatures (−25 °C) from chloroform (**2**) or from boiling *n*-pentane (**3**). Full lists of crystallographic refinement parameters and structure data for **2** and **3** are shown in Table 4.

The molecular structures of **2** (Fig. 4) and **3** (Fig. 5) confirm clearly the preference of C-alkylations *vs*. O-alkylations, which were predicted many years earlier [22, 36]. The C3≡C4 bond length of **2** is 1.181(2) Å, whereas the bond lengths of the single bonds C2–C3 (1.468(2) Å) and C4–C5 (1.461(2) Å) are shorter compared to that of C1–C2 (1.511(2) Å) and C5–C6 (1.513(2) Å). For **3**, the C1–C2 bond length is 1.480(4) Å. All bond lengths in **2** and **3** are shorter than a regular C–C bond length of sp^3-hybridized carbon atoms (1.54 Å). Due to the highly symmetrical cubic space group, the molecular structure of **3** shows a threefold axis along the C1–C2 bond. Hence, only one nitro group is included in the asymmetric unit while the others are symmetry generated, in an analogous manner as in the related structure of trinitromethane [54]. As expected, all nitro groups in **2** and **3** are planar. All bond lengths and angles were found in the range typical for polynitro aliphatic CHNO compounds, especially the elongated C–N bonds [54 – 57]. The trinitromethyl moieties show an approximate (for **2**) or true (for **3**) C_3 axis with propeller-like twisted nitro groups (Figs. 4 and 5) [55 – 57]. The nitro groups of **3** are rotated out of the CCN plane by 39.6°, which is slightly smaller than in trinitromethane [54]. For **2**, these C–C–N–O dihedral angles are in the range between 33.1 – 56.7°, quite common values for the trinitromethyl moiety without external perturbation [54 – 57]. This propeller-like twisting of the trinitromethyl moiety optimizes the non-bonded intramolecular N···O attractions between two adjacent nitro groups, while the corresponding O···O repulsions are minimized [56, 57]. These attractive N···O contacts were found in the range of

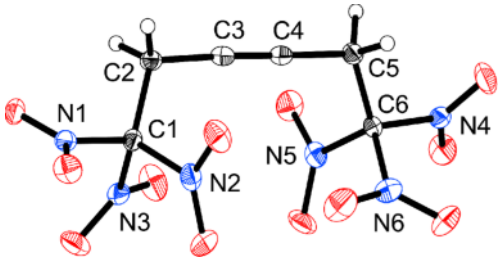

Fig. 4. Molecular structure of **2**. Selected distances (Å) and angles (deg): C1–N1 1.516(2), C1–N2 1.524(2), C1–N3 1.525(2), C1–C2 1.511(2), C2–C3 1.468(2), C3–C4 1.181(2), C4–C5 1.461(2), C5–C6 1.513(2), C6–N4 1.526(2), C6–N5 1.522(2), C6–N6 1.529(2); N1–C1–C2 111.0(2), N2–C1–C2 113.2(2), N3–C1–C2 113.6(2), C1–C2–C3 112.0(2), C2–C3–C4 176.7(2), C3–C4–C5 178.1(2), C4–C5–C6 112.9(2), C5–C6–N4 111.4(2), C5–C6–N5 112.9(2), C5–C6–N6 112.6(1).

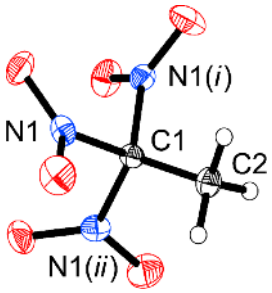

Fig. 5. Molecular structure of **3**. Selected distances (Å) and angles (deg): C1–C2 1.480(4), C1–N1/N1(*i*)/N1(*ii*) 1.529(2); C2–C1–N1/N1(*i*)/N1(*ii*) 113.4(1), N1–C1–N1(*i*)/N1(*ii*); N1(*i*)–C1–N1(*ii*) 105.3(1) (*i*: $-y$, $-0.5+z$, $0.5-x$; *ii*: $0.5-z$, $-x$, $0.5+y$).

2.54 – 2.60 Å (for **2**) and at 2.56 Å (for **3**), considerably lower than the sum of the van der Waals radii for nitrogen and oxygen (3.07 Å) [58]. The N–C–N angles of **2** and **3** are in the range 105.7 – 107.5° and therefore considerably smaller than the ideal tetrahedral value of 109.5° [54 – 57]. This is exactly the opposite of what is expected from steric interactions which would result in larger angles, but confirms the existence of N···O attractions within the trinitromethyl moiety [55].

The molecular structure of **2** reveals surprisingly the *cis*-isomer regarding the trinitromethyl moiety, which seems quite uncommon considering steric effects. The two trinitromethyl moieties are rotated against each other with a small torsion angle of 31.7° between the C1–C2 and C5–C6 bonds (Fig. 4), probably also due to attractive N···O interactions between the trinitromethyl

Table 4. Crystal and structure determination data for **2** and **3**.

	2	**3**
Formula	$C_6H_4N_6O_{12}$	$C_2H_3N_3O_6$
M_r, g mol^{-1}	352.13	165.06
Crystal size, mm^3	0.41 × 0.40 × 0.35	0.20 × 0.19 × 0.06
Crystal description	colorless block	colorless block
Crystal system	orthorhombic	cubic
Space group	*Pbca*	$I\bar{4}3d$
a, Å	12.9956(5)	13.6162(4)
b, Å	13.0433(4)	13.6162(4)
c, Å	15.1771(5)	13.6162(4)
V, Å^3	2572.6(2)	2524.5(2)
Z	8	16
$D_{calcd.}$, g cm^{-3}	1.82	1.74
Temperature, K	100(2)	100(2)
θ range, deg	3.75 – 26.00	4.73 – 25.99
μ(Mo K_α), mm^{-1}	0.2	0.2
F(000), e	1424	1344
hkl range	$-9 \le h \le +15$	$-7 \le k \le +16$
	$-18 \le l \le +10$	$-16 \le h \le +6$
	$-4 \le k \le +16$	$-11 \le l \le +9$
Refl. measured / independent / R_{int}	5183 / 2460 / 0.0209	1018 / 387 / 0.0251
Refl. "observed" with $I > 2\sigma(I)$	1703	306
Param. refined	217	38
$R(F)$ / $wR(F^2)$[a,b] [$I > 2\,\sigma(I)$]	0.0294 / 0.0575	0.0237 / 0.0337
$R(F)$ / $wR(F^2)$[a,b] (all refls.)	0.0490 / 0.0599	0.0355 / 0.0347
GoF (F^2)[c]	0.870	0.832
$\Delta\rho_{fin}$ (max / min), e Å^{-3}	0.238 / −0.214	0.124 / −0.107

[a] $R1 = \Sigma||F_o| - |F_c||/\Sigma|F_o|$; [b] $wR2 = [\Sigma w(F_o^2 - F_c^2)^2/\Sigma w(F_o^2)^2]^{1/2}$, $w = [\sigma^2(F_o^2) + (AP)^2 + BP]^{-1}$, where $P = (\mathrm{Max}(F_o^2, 0) + 2F_c^2)/3$ and A and B are constants adjusted by the program; [c] $\mathrm{GoF} = S = [\Sigma w(F_o^2 - F_c^2)^2/(n_{obs} - n_{param})]^{1/2}$, where n_{obs} is the number of data and n_{param} the number of refined parameters.

moieties. Although these N···O contacts (3.35/3.44 Å) are longer than the sum of the van der Waals radii (3.07 Å) [58], the partial charge distribution in nitro groups could lead to an appreciable Coulomb attraction. This proposal is supported by the fact that the oxygen atoms of one trinitromethyl moiety are pointing exactly towards the nitrogen atoms of the other moiety.

For steric reasons, in **3** the conformation of the hydrogen atoms and the nitro groups is staggered. The H–C1–C2–N1 dihedral angles are 53.8°/66.2°, compared to the ideal value of 60°. Each hydrogen atom of the methyl group in **3** is involved in one H···O interaction with two different adjacent molecules, leading to a total of three hydrogen bonds per molecule. This contact (2.60 Å) is only slightly shorter than the sum of the van der Waals radii (2.62 Å) [58] and consequently a weak interaction. The hydrogen atoms in **2** make a total of four hydrogen bonds to four adjacent molecules. Compared to **3**, these hydrogen bonds in the range 2.46 – 2.56 Å are slightly shorter.

Energetic properties

The DSC diagram of **3** shows three endothermic signals in the range of 25 – 400 °C. Beside the melting point at 53 °C and the boiling point at 194 °C (Table 5), an enantiotropic phase transition occurs at 39 °C. This polymorphism of **3** has previously been reported [59], as an example for the observation that compounds whose molecular shapes are nearly spherical show enantiotropic polymorphism [57, 60]. Furthermore, this molecular rotational freedom in the solid state leads to an unusual high melting point [60].

According to the UN recommendations [61], **1** and **2** are classified as very sensitive towards impact and friction, whereas **3** is classified as sensitive (*cf.* Table 5). Attempts to adsorb **1** on nitrocellulose to desensitize the material failed. This shows that the vapor pressure is too high for any standard application as double-based propellant.

Predictions of the detonation parameters using the EXPLO5 [62 – 65] code were made based on the ener-

Table 5. Energetic properties, calculated values and predicted detonation parameters of **1**–**3**.

	1	**2**	**3**
Chemical formula	$C_3H_3NO_3$	$C_6H_4N_6O_{12}$	$C_2H_3N_3O_6$
Formula weight, g mol^{-1}	101.06	352.13	165.06
N, %[a]	13.86	23.87	25.46
$N + O$, %[b]	61.35	78.39	83.62
Ω_{CO}, %[c]	−23.8	+18.2	+24.2
Ω_{CO_2}, %[d]	−71.2	−9.1	+4.9
Grain size, μm[e]	(liquid)	500 – 1000	500 – 1000
Impact, J[f]	1	3	8
Friction, N[g]	72	72	96
ESD, J[h]	–[l]	0.08	0.1
T_m, °C[i]	–	126	53
T_b / T_d, °C[j]	132 (dec.)	193 (dec.)	194 (boil.)
ρ, g cm^{-3}[k]	1.20 (est.)	1.818 (XRD)	1.737 (XRD)
H_{CBS-4M}, H[l]	−395.832687[2]	−1459.864955	−692.516945
	−395.831469[3]		
$\Delta H_f°$, kJ mol^{-1}[m]	114.68[2]	119.65	−120.36
	102.99[3]		
$\Delta U_f°$, kJ kg^{-1}[n]	1220.65[2]	417.23	−639.08
	1252.29[3]		
Q_v, kJ kg^{-1}[o]	−6990[2]	−7068	−6123
	−7020[3]		
T_{ex}, K[p]	4661[2]	5258	4615
	4676[3]		
p, kbar[q]	148[2]	351	309
	149[3]		
D, m s^{-1}[r]	6613[2]	8535	8306
	6622[3]		
V_0, L kg^{-1}[s]	679[2]	625	711
	679[3]		
I_s, s^{-1}[t]	260[2]	274	262
	261[3]		

[a] Nitrogen content; [b] combined nitrogen and oxygen content; [c] oxygen balance assuming the formation of CO; [d] oxygen balance assuming the formation of CO_2; [e] grain size of the samples used for sensitivity tests; [f] impact sensitivity; [g] friction sensitivity; [h] sensitivity towards electrostatic discharge; [i] melting point; [j] boiling (boil.) or decomposition (dec.) point; [k] density estimated (est.) or calculated from X-ray diffraction (XRD); [l] enthalpy derived from quantum-chemical CBS-4M calculation; [m] enthalpy of formation (calculated); [n] energy of formation (calculated); [o] detonation energy (calculated); [p] explosion temperature (calculated); [q] detonation pressure (calculated); [r] detonation velocity (calculated); [s] gas volume (calculated, assuming only gaseous products); [t] specific impulse (calculated isobaric combustion with 100 % **1**, **2** or **3** at 70 kbar chamber pressure, equilibrium expansion against 1.0 bar ambient pressure). [l] Not determined (ESD test not measurable for liquids); [2] *gauche*-propargyl nitrate; [3] *anti*-propargyl nitrate.

gies of formation, calculated *ab inito* using the GAUSSIAN 09 program package [66]. The energetic properties, calculated detonation parameters as well as further calculated energies and enthalpies of formation of **1**–**3** are shown in Table 5.

Conclusion

The structures of *anti*- and *gauche*-propargyl nitrate (**1**) in the gas phase have been determined by electron diffraction, and that of hexanitrohex-3-yne (**2**) and 1,1,1-trinitroethane (**3**) in the crystalline state by X-ray diffraction. A vapor composition with 69(2) % *anti*-conformer was found in the GED experiment for **1** – in good agreement with relative conformer energy values from *ab initio* calculations. The structural parameters resulting from the GED date are also in good agreement with computational values. A propeller type twisting of the trinitromethyl moieties is present in the crystal structures of both **2** and **3** because of N···O interactions. Furthermore, an NMR study (^{109}Ag and ^{14}N) of the important precursor silver

trinitromethanide in various solvents was performed and showed significant differences in the corresponding chemical shifts.

Experimental Section

General procedures

All manipulation of air- and moisture-sensitive materials were performed under an inert atmosphere of dry nitrogen using flame-dried glass vessels and Schlenk techniques [67]. Due to the light sensitivity of silver salts, reactions with silver acetate and silver carbonate were performed under the absence of light. The solvents and silver acetate (Fluka), silver carbonate (ABCR), and iodomethane (Acros Organics) were used as received. The aqueous solution of trinitromethane (Aerospace Propulsion Products B.V.) was extracted and purified by precipitation of its potassium salt and subsequent acidification. 1,4-Dibromobut-2-yne was synthesized according to the literature procedure [68]. Raman spectra were recorded with a Bruker MultiRAM FT-Raman instrument fitted with a liquid nitrogen cooled germanium detector and a Nd:YAG laser (λ = 1064 nm, 300 mW). Infrared (IR) spectra were measured with a Perkin-Elmer Spectrum BX-FTIR spectrometer equipped with a Smiths DuraSampl*IR* II ATR device. All spectra were recorded at ambient temperature, the samples were neat solids. NMR spectra were recorded at 25 °C with a Jeol Eclipse 400 instrument, and chemical shifts were determined with respect to external Me_4Si (^1H, 400.2 MHz; ^{13}C, 100.6 MHz), $MeNO_2$ (^{14}N, 29.0 MHz; ^{15}N, 40.6 MHz), and 0.5M $AgNO_3$ in D_2O (^{109}Ag, 18.6 MHz). Mass spectrometric data were obtained with a Jeol MStation JMS 700 spectrometer (DEI+, DCI+). The fragments are referred to the isotope with the highest natural abundance. Elemental analyses (C/H/N) were performed with a Elementar vario EL analyzer. Melting points and decomposition points were determined by differential scanning calorimetry (DSC) measurements with a Linseis DSC-PT10 apparatus, using a heating rate of 5 °C min^{-1}. Sensitivity data (impact, friction, and electrostatic discharge) were performed using a drophammer, friction tester, and electrostatic discharge device conform to the directive of the Federal Institute for Materials Research and Testing (BAM) [69].

Computational methods

Hartree-Fock (HF) calculations were of the restricted type and the second-order Møller-Plesset (MP2) calculations made use of the resolution-of-the-identity (RI) method and the default frozen-core partitioning as implemented in TURBOMOLE (version 5.7) [70]. The DFT calculation using 6-311++G** type basis sets and the B3LYP functional were performed using the default criteria in GAUSSIAN 03 (revision C.02) [71], whilst those using the def2-TZVPP (herein shortened to TZVPP) basis set were performed using TURBOMOLE (version 5.7).

Gas electron diffraction (GED)

Electron scattering intensities were recorded at room temperature on a combination of reusable Fuji and Kodak imaging plates using a Balzers KD-G2 Gas-Eldigraph [72, 73]. This device was equipped with an electron source built by STAIB Instruments, and was operated at 60 kV when recording data. The accelerating voltage was stable to within 1 to 2 V during the course of the experiment. The image plates were scanned using a Fuji BAS 1800 II scanner, yielding digital 16-bit grey-scale image data. Further details about the Bielefeld GED apparatus and the experimental methods are published elsewhere [48].

In preparation for data reduction, the long and short nozzle-to-plate distances were re-measured after recording the short-distance data and before recording the long-distance data. The relative scaling of the two scanning directions was recalibrated using an exposed image plate with two pairs of pin holes, which was scanned in two orientations, approximately perpendicular to one another. The data were reduced to total intensities using PIMAG (version 040827) [74] in connection with a sector curve, which was based on experimental xenon scattering data and tabulated scattering factors of xenon. Further data reduction yielding molecular intensity curves was performed using the ED@ED program (Version 3.0) [75] and scattering factors [76]. For both compounds the ratio of the electron wavelength to the nozzle-to-plate distances was checked using benzene data and the widely accepted r_a value of 1.397 Å for the C–C distance in benzene. The data reduction was performed using indirectly determined nozzle-to-plate distances. The electron wavelengths and nozzle-to-plate distances are provided as Supplementary Information, along with other data analysis parameters including the *s* limits, weighting points, *R* factors (R_D and R_G), scale factors, data correlation values and the correlation matrix.

The amplitudes of vibration, *u*, used in r_e (by approximated anharmonic corrections implemented as $r_{a3,1}$ in ED@ED) refinement and the anharmonic distance corrections were calculated using the program SHRINK [51, 53]. This made use of anharmonic force field calculations at the B3LYP/6-311++G** level of theory (see above for details of computational methods). The SHRINK input files were generated using Q2SHRINK [77].

Energetic properties

All quantum chemical calculations for the prediction of the energetic properties were carried out using the program package GAUSSIAN 09 (revision C.01) [66], additionally prepared and visualized with GAUSSVIEW 5 (ver-

sion 5.0.8) [78]. The initial geometries of the structures were taken from the corresponding experimentally determined crystal structures. The enthalpies (H) and free energies (G) were calculated using the complete basis set (CBS) method in order to obtain very accurate values [79 – 82]. This method is a complex energy computation involving several pre-defined calculations on the specified system. The used method CBS-4M ('M' referring to the use of minimal population localization) is an updated version of the modified CBS-4 method [83, 84] with both the new localization procedure and improved empirical parameters [84]. The liquid (**1**) and solid (**2**, **3**) state enthalpies and energies of formation were calculated from the corresponding enthalpy derived from these quantum-chemical CBS-4M calculations (H_{CBS-4M}). Therefore, the enthalpies of formation of the gas-phase species were computed according to the atomization energy method [85 – 87]. The liquid (solid) state energies of formation (ΔH_f°) were estimated by subtracting the gas-phase enthalpies with the corresponding enthalpy of vaporization (sublimation) obtained by Trouton's rule [88, 89]. These enthalpies of formation were used to calculate the energies of formation (ΔU_f°). The calculation of the detonation parameters were performed using the program EXPLO5 (version 5.05) [62 – 65]. The input was made using the sum formula, the liquid respectively solid-state energies of formation and the experimentally determined densities, derived from the corresponding single-crystal X-ray structures.

X-Ray crystallography

For both compounds, an Oxford Xcalibur3 diffractometer with a CCD area detector was employed for data collection using MoK_α radiation (λ = 0.71073 Å). The structures were solved using Direct Methods (SIR2004) [90, 91] and refined by full-matrix least-squares on F^2 (SHELXL-97) [92, 93]. All non-hydrogen atoms were refined anisotropically. The hydrogen atoms were located in difference Fourier maps and placed with a C–H distance of 0.99 Å for CH_2 groups, C–H distances for the CH_3 group were refined. ORTEP plots are shown with thermal ellipsoids at the 50 % probability level.

CCDC 900037 (**2**), and 900038 (**3**) contain the supplementary crystallographic data for this paper. These data can be obtained free of charge from The Cambridge Crystallographic Data Centre *via* www.ccdc.cam.ac.uk/data_request/cif.

CAUTION! All compounds with a high nitrogen and oxygen content are potentially explosive energetic materials. Furthermore, many alkyl nitrates are extremely sensitive; therefore they must be handled with care. This necessitates additional meticulous safety precautions (steel-reinforced Kevlar® gloves, Kevlar® sleeves, face shield, leather coat, and ear plugs). Only earthened and metal-free equipment was used during the synthesis.

*Synthesis of propargyl nitrate (**1**)*

A nitration mixture consisting of 10.0 mL of acetic anhydride (91 mmol) and 3.3 mL of nitric acid (79 mmol) is cooled to −10 °C, and 3.7 mL of propargyl alcohol (68 mmol) is added dropwise at such a rate, that the temperature does not exceed −5 °C. Stirring is continued for 1 h and the reaction mixture is allowed to warm to ambient temperature. After pouring on ice the yellowish oil is separated immediately. The oily liquid is dissolved in 20 mL of dichloromethane and treated with a saturated aqueous solution of $NaHCO_3$, until the gas evolution ceases. The organic phase is washed with water (2 × 25 mL) and a saturated aqueous solution of NaCl and dried over anhydrous $MgSO_4$. Concentration *in vacuo* afforded 4.0 g (39 mmol) of crude propargyl nitrate (58 %), which was further purified by careful condensation at 25 °C using dry ice cooling. – Raman: ν = 2961 (44), 2134 (100, νC≡C), 1643 (5, $\nu_{as}NO_2$), 1427 (11), 1361 (11), 1281 (34, ν_sNO_2), 921 (13), 848 (23), 613 (14), 474 (11), 431 (12), 296 (27), 221 (19) cm^{-1}. – IR: ν = 3327 (m), 2952 (w), 2560 (w), 2137 (w, νC≡C), 1776 (w), 1748 (w), 1677 (vs, $\nu_{as}NO_2$), 1434 (m), 1365 (m), 1284 (vs, ν_sNO_2), 1230 (w), 1071 (w), 1017 (s), 976 (m), 927 (m), 839 (s), 757 (w), 675 (m), 639 (m), 596 (w), 471 (w) cm^{-1}. – ^{1}H NMR ($CDCl_3$): δ = 4.96 (d, $^4J_{H-H}$ = 2.2 Hz, 2 H, CH_2), 2.59 (t, CH). – ^{13}C{^{1}H} NMR ($CDCl_3$): δ = 76.8 (s, CCH$_2$), 74.7 (s, CH), 59.9 (s, CH$_2$). – ^{15}N NMR ($CDCl_3$): δ = −47.1 (t, $^3J_{N-H}$ = 4.4 Hz, ONO$_2$). – MS (DEI+): m/z (%) = 100 (21) [M–H]$^+$. – HRMS: m/z (%) = 101.0113 (100) [M]$^+$. – DSC (T_{onset}, 5 K min^{-1}): 132 °C (decomposition). – Sensitivities (liquid): impact sensitivity: 1 J, friction sensitivity: 72 N.

*Synthesis of 1,1,1,6,6,6-hexanitrohex-3-yne (**2**)*

The synthesis was performed according to the literature procedure [14]. – Raman: ν = 2972 (30), 2937 (79), 2343 (9), 2305 (15), 2264 (44, νC≡C), 1614 (17), 1598 (21, $\nu_{as}NO_2$), 1407 (25), 1365 (43), 1324 (24), 1307 (36, ν_sNO_2), 1250 (6), 1170 (3), 1142 (4), 1003 (20), 859 (100, νCN), 831 (4), 807 (6), 775 (5), 723 (5), 642 (7), 561 (6), 546 (19), 445 (4), 406 (55), 371 (70), 310 (20), 289 (47), 233 (15), 223 (10), 196 (11) cm^{-1}. – IR: ν = 2970 (m), 2936 (m), 2892 (w), 1581 (vs, $\nu_{as}NO_2$), 1404 (m), 1365 (m), 1300 (s, ν_sNO_2), 1262 (m), 1249 (m), 1214 (w), 1169 (w), 1140 (w), 1128 (w), 1021 (w), 863 (m), 857 (m,νCN), 829 (w), 804 (s), 772 (m), 720 (w), 668 (w), 640 (w) cm^{-1}. – ^{1}H NMR ($CDCl_3$): δ = 3.99 (s, 4 H, CH_2). – ^{13}C{^{1}H} NMR ($CDCl_3$): δ = 124.8 (br, C(NO$_2$)$_3$), 74.3 (s, CCH$_2$), 26.8 (s, CH$_2$). – ^{15}N NMR ($CDCl_3$): δ = −33.9 (s, NO$_2$). – EA for $C_6H_4N_6O_{12}$ (352.13): calcd. C 20.47, H 1.14, N 23.87; found C 20.48, H 1.23, N 22.99 %. – DSC (T_{onset}, 5 K min^{-1}): 126 °C (melting point), 193 °C (decomposition). – Sensitivities (grain size: 500 – 1000 μm): impact sen-

sitivity: 3 J, friction sensitivity: 72 N, electrostatic sensitivity: 0.08 J.

*Synthesis of 1,1,1-trinitroethane (**3**)*

Into a suspension of silver carbonate (2.12 g, 7.68 mmol) in 5 mL of acetonitrile is added an aqueous solution (30 %) of trinitromethane (2.31 g, 15.3 mmol) at ambient temperature. After stirring the yellow reaction mixture containing the *in situ* formed silver trinitromethanide for 25 min, iodomethane (2.17 g, 15.3 mmol) is added dropwise, with stirring continued for additional 15 h. The pale yellow precipitate of silver iodide is filtered off. Removing of the solvent *in vacuo* left a light-yellow solid. Crystallization of the product from *n*-pentane yielded 1.59 g (63 %) of **3** as colorless crystals.

WARNING! If, instead of an aqueous solution of trinitromethane, the trinitromethane is applied in a neat (anhydrous) form, after immediate evaporation of the solvent acetonitrile (5 min), the residue explodes reproducibly and can result in serious damage. Longer reaction times (*ca.* 30 min) result in significant decomposition of $Ag[C(NO_2)_3]$ to silver nitrate. – Raman: ν = 3032 (35), 2957 (68), 1613 (10), 1600 (37, $\nu_{as}NO_2$), 1436 (13), 1395 (30), 1359 (34), 1313 (24, ν_sNO_2), 1177 (7), 1133 (10), 885 (20), 858 (100, νCN), 784 (14), 713 (5), 643 (14), 530 (34), 412 (62), 383 (73), 319 (28) cm^{-1}. – IR: ν = 3032 (m), 2956 (w), 2900 (w), 1587 (vs, $\nu_{as}NO_2$), 1434 (m), 1392 (s), 1307 (s, ν_sNO_2), 1266 (m), 1176 (m), 1131 (s), 881 (s), 858 (m, νCN), 782 (vs), 711 (w) cm^{-1}. – ^{1}H NMR ($CDCl_3$): δ = 2.76 (s, 3 H, CH_3). – $^{13}C\{^1H\}$ NMR ($CDCl_3$): δ = 128.2 (septet, $^1J_{C-14N}$ = 8.1 Hz, $C(NO_2)_3$), 21.1 (s, CH_3). – ^{15}N NMR ($CDCl_3$): δ = −28.8 (q, $^3J_{N-H}$ = 2.7 Hz, NO_2). – MS (DCI+): *m/z* (%) = 166 (5) $[M]^+$, 120 (5) $[M–NO_2]^+$, 73 (1) $[M–2\ NO_2]^+$, 46 (52) $[NO_2]^+$, 27 (100) $[M–3\ NO_2]^+$. – EA for $C_2H_3N_3O_6$ (165.06): calcd. C 14.55, H 1.83, N 25.46; found C 14.51, H 1.88, N 25.04 %. – DSC (T_{onset}, 5 K min^{-1}): 38 °C (transition temperature) 53 °C (melting point), 194 °C (boiling point). – Sensitivities (grain size: 500 – 1000 μm): impact sensitivity: 8 J, friction sensitivity: 96 N, electrostatic sensitivity: 0.10 J.

Supporting information

^{15}N NMR and vibrational (IR and Raman) spectra and further details of the GED determination of **1** are given as Supporting Information available online (DOI: 10.5560/ZNB.2013-2311).

Acknowledgement

Deutsche Forschungsgemeinschaft (GED grant MI477/10-1) is gratefully acknowledged. Financial support of this work is provided by the Ludwig-Maximilian University of Munich (LMU) and the U. S. Army Research Laboratory (ARL) under grant no. W911NF-09-2-0018. The authors acknowledge collaboration with Dr. Mila Krupka (OZM Research, Czech Republic) in the development of new testing and evaluation methods for energetic materials and with Dr. Muhamed Sucesca (Brodarski Institute, Croatia) in the development of new computational codes to predict the detonation and propulsion parameters of novel explosives. Dominik Baumann, M. Sc., and Matthias Trunk, M. Sc., are thanked for their participation within this project.

[1] T. Urbanski, *Chemistry and Technology of Explosives*, Vol. 4, Pergamon Press, Oxford, **1984**.
[2] F. P. Bowden, A. D. Yoffe, *Initiation and Growth of Explosion in Liquids and Solids*, Cambridge University Press, Cambridge, **1952**.
[3] F. P. Bowden, A. D. Yoffe, *Fast Reactions in Solids*, Butterworths Scientific Publications, London, **1958**.
[4] T. Urbanski, W. Tarantowicz, *B. Acad. Pol. Sci., Geo. G.* **1958**, *6*, 289 – 292.
[5] M. S. Cohen, D. D. Perry, P. J. Keenan, US3120566, **1964**.
[6] P. Klaeboe, C. J. Nielsen, H. Priebe, S. H. Schei, C. E. Sjoegren, *J. Mol. Struct.* **1986**, *141*, 161 – 172.
[7] A. Quilico, M. Freri, *Gazz. Chim. Ital.* **1929**, *59*, 930 – 941.
[8] A. Quilico, M. Freri, *Gazz. Chim. Ital.* **1930**, *60*, 172 – 184.
[9] A. Quilico, M. Freri, *Gazz. Chim. Ital.* **1930**, *60*, 721 – 744.
[10] V. A. Quilico, M. Freri, *Gazz. Chim. Ital.* **1931**, *61*, 484 – 500.
[11] A. Quilico, M. Simonetta, *Gazz. Chim. Ital.* **1946**, *76*, 200 – 214.
[12] A. Quilico, M. Simonetta, *Gazz. Chim. Ital.* **1946**, *76*, 255 – 264.
[13] A. D. Nikolaeva, A. P. Kirsanov, R. G. Kadyrova, *Izv. Vyssh. Uchebn. Zaved., Khim. Khim. Tekhnol.* **1975**, *18*, 1715 – 1716.
[14] P. O. Tawney, US3040105, **1962**.
[15] S. G. Cho, K. T. No, E. M. Goh, J. K. Kim, J. H. Shin, Y. D. Joo, S. Seong, *Bull. Korean Chem. Soc.* **2005**, *26*, 399 – 408.
[16] M. H. Keshavarz, H. R. Pouretedal, *J. Hazard. Mater.* **2005**, *124*, 27 – 33.
[17] N. R. Badders, C. Wei, A. A. Aldeeb, W. J. Rogers, M. S. Mannan, *J. Energ. Mater.* **2006**, *24*, 17 – 33.
[18] M. H. Keshavarz, *J. Hazard. Mater.* **2007**, *148*, 648 – 652.

[19] J. A. Morrill, E. F. C. Byrd, *J. Mol. Graphics Modell.* **2008**, *27*, 349 – 355.
[20] A. P. N. Franchimont, *Rec. Trav. Chim. Pay-Bas.* **1886**, *5*, 281 – 289.
[21] A. Hantzsch, A. Rinckenberger, *Ber. Dtsch. Chem. Ges.* **1899**, *32*, 628 – 641.
[22] A. Hantzsch, K. S. Caldwell, *Ber. Dtsch. Chem. Ges.* **1906**, *39*, 2472 – 2478.
[23] G. S. Hammond, W. D. Emmons, C. O. Parker, B. M. Graybill, J. H. Waters, M. F. Hawthorne, *Tetrahedron* **1963**, *19*, 177 – 195.
[24] C. W. Plummer, US3049570, **1962**.
[25] F. M. Mukhametshin, V. D. Surkov, A. L. Fridman, F. A. Gabitov, SU515738, **1976**.
[26] N. N. Makhova, I. V. Ovchinnikov, V. G. Dubonos, Y. A. Strelenko, L. I. Khmel'nitsky, *Russ. Chem. Bull.* **1993**, *42*, 131 – 136.
[27] C. F. Poranski, Jr., W. B. Moniz, *J. Phys. Chem.* **1967**, *71*, 1142 – 1143.
[28] J. P. Kintzinger, J. M. Lehn, R. L. Williams, *Mol. Phys.* **1969**, *17*, 135 – 146.
[29] M. Witanowski, Z. Biedrzycka, K. Grela, *Magn. Reson. Chem.* **1998**, *36*, 356 – 358.
[30] M. Witanowski, Z. Biedrzycka, K. Grela, K. Wejroch, *Magn. Reson. Chem.* **1998**, *36*, S85–S92.
[31] H. Wittek, *Acta Phys. Austriaca* **1948**, *1*, 303 – 306.
[32] E. M. Popov, *J. Struct. Chem.* **1967**, *8*, 916 – 918.
[33] J. T. Larkins, F. E. Saalfeld, L. Kaplan, *Org. Mass Spectrom.* **1969**, *2*, 213 – 221.
[34] J. T. Larkins, J. M. Nicholson, F. E. Saalfeld, *Org. Mass Spectrom.* **1971**, *5*, 265 – 277.
[35] O. S. Chizhov, V. I. Kadentsev, G. G. Pal'mbakh, K. Y. Burshtein, S. A. Shevelev, A. A. Fainzil'berg, *Org. Mass Spectrom.* **1978**, *13*, 611 – 617.
[36] K. V. Auwers, L. Harres, *Ber. Dtsch. Chem. Ges.* **1929**, *62B*, 2287 – 2297.
[37] T. M. Klapötke, B. Krumm, R. Moll, *New Trends Res. Energ. Mater., 14th Proc. Semin.*, Pardubice (Czech Republic) **2011**, Pt. 2, pp. 723 – 729.
[38] F. S. Holahan, T. C. Castorina, J. R. Autera, S. Helf, *J. Am. Chem. Soc.* **1962**, *84*, 756 – 759.
[39] V. I. Erashko, V. I. Slovetskii, S. A. Shevelev, A. A. Fainzil'berg, *Russ. Chem. Bull.* **1971**, *20*, 645 – 649.
[40] N. Kornblum, R. A. Smiley, R. K. Blackwood, D. C. Iffland, *J. Am. Chem. Soc.* **1955**, *77*, 6269 – 6280.
[41] S. A. Shevelev, V. I. Erashko, A. A. Fainzil'berg, *Russ. Chem. Bull.* **1968**, *17*, 447.
[42] S. A. Shevelev, V. I. Erashko, A. A. Fainzil'berg, *Russ. Chem. Bull.* **1968**, *17*, 2003 – 2006.
[43] V. I. Erashko, S. A. Shevelev, A. A. Fainzil'berg, *Russ. Chem. Bull.* **1968**, *17*, 2007 – 2010.
[44] M. Göbel, T. M. Klapötke, P. Mayer, *Z. Anorg. Allg. Chem.* **2006**, *632*, 1043 – 1050.
[45] A. L. Fridman, T. N. Ivshina, V. P. Ivshin, V. A. Tartakovskii, S. S. Novikov, *Russ. Chem. Bull.* **1969**, *18*, 2193 – 2194.
[46] R. G. Kidd, "Nuclear Shielding of the Transition Metals" in *Annual Reports on NMR Spectroscopy*, Vol. 10A (Ed.: G. A. Webb), Academic Press Inc., London, **1980**, pp. 53 – 55.
[47] W. W. Simons, *The Sadtler Handbook of Infrared Spectra*, Sadtler Research Laboratories, Philadelphia, **1978**, p. 3.
[48] R. J. F. Berger, M. Hoffmann, S. A. Hayes, N. W. Mitzel, *Z. Naturforsch.* **2009**, *64b*, 1259 – 1268.
[49] A. J. Blake, P. T. Brain, H. McNab, J. Miller, C. A. Morrison, S. Parsons, D. W. H. Rankin, H. E. Robertson, B. A. Smart, *J. Phys. Chem.* **1996**, *100*, 12280 – 12287.
[50] N. W. Mitzel, D. W. H. Rankin, *Dalton Trans.* **2003**, 3650 – 3662.
[51] V. A. Sipachev, *J. Mol. Struct.: THEOCHEM* **1985**, *22*, 143 – 151.
[52] D. W. H. Rankin in *Stereochemical Applications of Gas-Phase Electron Diffraction*, Vol. 1 (Eds.: I. Hargittai, M. Hargittai), John Wiley & Sons, New York, **1988**, pp. 451 – 482.
[53] V. P. Novikov, V. A. Sipachev, E. I. Kulikova, L. V. Vilkov, *J. Mol. Struct.* **1993**, *301*, 29 – 36.
[54] H. Schödel, R. Dienelt, H. Bock, *Acta Crystallogr.* **1994**, *C50*, 1790 – 1792.
[55] S. K. Bhattacharjee, H. L. Ammon, *Acta Crystallogr.* **1982**, *B38*, 2503 – 2505.
[56] Y. Oyumi, T. B. Brill, A. L. Rheingold, *J. Phys. Chem.* **1985**, *89*, 4824 – 4828.
[57] T. M. Klapötke, B. Krumm, R. Moll, S. F. Rest, *Z. Anorg. Allg. Chem.* **2011**, *637*, 2103 – 2110.
[58] A. Bondi, *J. Phys. Chem.* **1964**, *68*, 441 – 451.
[59] J. M. Rosen, *Microscope* **1969**, *17*, 141 – 144.
[60] R. W. Crowe, C. P. Smyth, *J. Am. Chem. Soc.* **1950**, *72*, 4009 – 4015.
[61] T. M. Klapötke, *Chemistry of High-Energy Materials*, 2nd ed., Walter de Gruyter, Berlin, **2012**.
[62] M. Suceska, *Propellants, Explos., Pyrotech.* **1991**, *16*, 197 – 202.
[63] M. Suceska, *Propellants, Explos., Pyrotech.* **1999**, *24*, 280 – 285.
[64] M. Suceska, *Mater. Sci. Forum* **2004**, *465 – 466*, 325 – 330.
[65] M. Suceska, EXPLO5 (version 5.05), Brodarski Institut, Zagreb (Croatia), **2011**.
[66] M. J. Frisch, G. W. Trucks, H. B. Schlegel, G. E. Scuseria, M. A. Robb, J. R. Cheeseman, V. B. G. Scalmani, B. Mennucci, G. A. Petersson, H. Nakatsuji, M. Caricato, X. Li, H. P. Hratchian, A. F. Izmaylov, J. Bloino, G. Zheng, J. L. Sonnenberg, M. Hada, M. Ehara, K. Toyota, R. Fukuda, J. Hasegawa, M. Ishida, T. Naka-

jima, Y. Honda, O. Kitao, H. Nakai, T. Vreven, J. A. Montgomery, Jr., J. E. Peralta, F. Ogliaro, M. Bearpark, J. J. Heyd, E. Brothers, K. N. Kudin, V. N. Staroverov, R. Kobayashi, J. Normand, K. Raghavachari, A. Rendell, J. C. Burant, S. S. Iyengar, J. Tomasi, M. Cossi, N. Rega, J. M. Millam, M. Klene, J. E. Knox, J. B. Cross, V. Bakken, C. Adamo, J. Jaramillo, R. Gomperts, R. E. Stratmann, O. Yazyev, A. J. Austin, R. Cammi, C. Pomelli, J. W. Ochterski, R. L. Martin, K. Morokuma, V. G. Zakrzewski, G. A. Voth, P. Salvador, J. J. Dannenberg, S. Dapprich, A. D. Daniels, Ö. Farkas, J. B. Foresman, J. V. Ortiz, J. Cioslowski, D. J. Fox, GAUSSIAN 09 (rev. C.01), Gaussian, Inc., Wallingford CT (USA), **2009**.

[67] D. F. Shriver, M. A. Drezdzon, *The Manipulation of Air-Sensitive Compounds*, 2nd ed., John Wiley & Sons, New York, **1986**.

[68] M. Saljoughian, H. Morimoto, P. G. Williams, H. Rapoport, *J. Labelled Compd. Radiopharm.* **1988**, *25*, 313 – 328.

[69] Test procedure *A.14 Explosive Properties* according to Council Regulation (EC) No 440/2008 of 30 May 2008 laying down test methods pursuant to Regulation (EC) No 1907/2006 of the European Parliament and of the Council on the Registration, Evaluation, Authorisation and Restriction of Chemicals (REACH), *OJ L 142*, 93 – 103, **2008**.

[70] R. Ahlrichs, M. Baer, M. Haeser, H. Horn, C. Koelmel, *Chem. Phys. Lett.* **1989**, *162*, 165 – 169.

[71] M. J. Frisch, G. W. Trucks, H. B. Schlegel, G. E. Scuseria, M. A. Rob, J. R. Cheeseman, J. A. Montgomery Jr. T. Vreven, K. N. Kudin, J. C. Burant, J. M. Millam, S. S. Iyengar, J. Tomasi, V. Barone, B. Mennucci, M. Cossi, G. Scalmani, N. Rega, G. A. Petersson, H. Nakatsuji, M. Hada, M. Ehara, K. Toyota, R. Fukuda, J. Hasegawa, M. Ishida, T. Nakajima, Y. Honda, O. Kitao, H. Nakai, M. Klene, X. Li, J. E. Knox, H. P. Hratchian, J. B. Cross, V. Bakken, C. Adamo, J. Jaramillo, R. Gomperts, R. E. Stratmann, O. Yazyev, A. J. Austin, R. Cammi, C. Pomelli, J. W. Ochterski, P. Y. Ayala, K. Morokuma, G. A. Voth, P. Salvador, J. J. Dannenberg, V. G. Zakrzewski, S. Dapprich, A. D. Daniels, M. C. Strain, O. Farkas, D. K. Malick, A. D. Rabuck, K. Raghavachari, J. B. Foresman, J. V. Ortiz, Q. Cui, A. G. Baboul, S. Clifford, J. Cioslowski, B. B. Stefanov, G. Liu, A. Liashenko, P. Piskorz, I. Komaromi, R. L. Martin, D. J. Fox, T. Keith, M. A. Al-Laham, C. Y. Peng, A. Nanayakkara, M. Challacombe, P. M. W. Gill, B. Johnson, W. Chen, M. W. Wong, C. Gonzalez, J. A. Pople, GAUSSIAN 03 (rev. B.03), Gaussian, Inc., Wallingford CT (USA), **2003**.

[72] W. Zeil, J. Haase, L. Wegmann, *Z. Instrumentenkd.* **1966**, *74*, 84 – 88.

[73] H. Oberhammer, *Mol. Struct. Diffr. Methods* **1976**, *4*, 24 – 44.

[74] S. Gundersen, S. Samdal, T. G. Strand, H. V. Volden, *J. Mol. Struct.* **2007**, *832*, 164 – 171.

[75] S. L. Hinchley, H. E. Robertson, K. B. Borisenko, A. R. Turner, B. F. Johnston, D. W. H. Rankin, M. Ahmadian, J. N. Jones, A. H. Cowley, *Dalton Trans.* **2004**, 2469 – 2476.

[76] A. W. Ross, M. Fink, R. Hilderbrandt in *International Tables for Crystallography*, Vol. C (Ed.: A. J. C. Wilson), Kluwer Academic Publishers, Dordrecht, **1992**, p. 245.

[77] A. V. Zakharov, Y. A. Zhabanov, Q2SHRINK ED Software, http://edsoftware.sourceforge.net.

[78] R. D. Dennington II, T. A. Keith, J. M. Millam, GAUSSVIEW (version 5.0.8), Semichem Inc., Shawnee Mission KS (USA), **2009**.

[79] M. R. Nyden, G. A. Petersson, *J. Chem. Phys.* **1981**, *75*, 1843 – 1862.

[80] G. A. Petersson, M. A. Al-Laham, *J. Chem. Phys.* **1991**, *94*, 6081 – 6090.

[81] G. A. Petersson, T. G. Tensfeldt, J. A. Montgomery, Jr., *J. Chem. Phys.* **1991**, *94*, 6091 – 6101.

[82] J. A. Montgomery, Jr., J. W. Ochterski, G. A. Petersson, *J. Chem. Phys.* **1994**, *101*, 5900 – 5909.

[83] J. W. Ochterski, G. A. Petersson, J. A. Montgomery, Jr., *J. Chem. Phys.* **1996**, *104*, 2598 – 2619.

[84] J. A. Montgomery, Jr., M. J. Frisch, J. W. Ochterski, G. A. Petersson, *J. Chem. Phys.* **2000**, *112*, 6532 – 6542.

[85] L. A. Curtiss, K. Raghavachari, P. C. Redfern, J. A. Pople, *J. Chem. Phys.* **1997**, *106*, 1063 – 1079.

[86] B. M. Rice, S. V. Pai, J. Hare, *Combust. Flame* **1999**, *118*, 445 – 458.

[87] E. F. C. Byrd, B. M. Rice, *J. Phys. Chem.* **2006**, *110A*, 1005 – 1013.

[88] F. Trouton, *Philos. Mag.* **1884**, *18*, 54 – 57.

[89] M. S. Westwell, M. S. Searle, D. J. Wales, D. H. Williams, *J. Am. Chem. Soc.* **1995**, *117*, 5013 – 5015.

[90] M. C. Burla, R. Caliandro, M. Camalli, B. Carrozzini, G. L. Cascarano, L. de Caro, C. Giacovazzo, G. Polidori, R. Spagna, SIR2004, An Improved Tool for Crystal Structure Determination and Refinement, University of Bari, Bari (Italy), **2004**.

[91] M. C. Burla, R. Caliandro, M. Camalli, B. Carrozzini, G. L. Cascarano, L. de Caro, C. Giacovazzo, G. Polidori, R. Spagna, *J. Appl. Crystallogr.* **2005**, *38*, 381 – 388.

[92] G. M. Sheldrick, SHELXL-97, Program for the Refinement of Crystal Structures, University of Göttingen, Göttingen (Germany) **1997**.

[93] G. M. Sheldrick, *Acta Crystallogr.* **2008**, *A64*, 112 – 122.